



HAL
open science

Plume-induced dynamic instabilities near cratonic blocks: implications for P-T-t paths and metallogeny

Laurent Guillou-Frottier, Evgenii E.B. Burov, Sierd Cloetingh, Elisabeth Le Goff, Yves Deschamps, Benjamin Huet, Vincent Bouchot

► To cite this version:

Laurent Guillou-Frottier, Evgenii E.B. Burov, Sierd Cloetingh, Elisabeth Le Goff, Yves Deschamps, et al.. Plume-induced dynamic instabilities near cratonic blocks: implications for P-T-t paths and metallogeny. *Global and Planetary Change*, 2012, 90-91, pp.37-50. 10.1016/j.gloplacha.2011.10.007 . hal-00634433

HAL Id: hal-00634433

<https://brgm.hal.science/hal-00634433>

Submitted on 21 Oct 2011

HAL is a multi-disciplinary open access archive for the deposit and dissemination of scientific research documents, whether they are published or not. The documents may come from teaching and research institutions in France or abroad, or from public or private research centers.

L'archive ouverte pluridisciplinaire **HAL**, est destinée au dépôt et à la diffusion de documents scientifiques de niveau recherche, publiés ou non, émanant des établissements d'enseignement et de recherche français ou étrangers, des laboratoires publics ou privés.

Accepted Manuscript

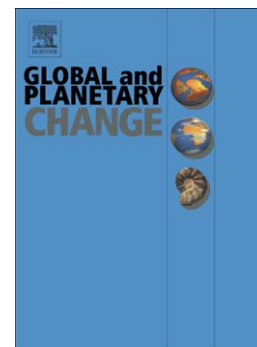
Plume-induced dynamic instabilities near cratonic blocks: Implications for P-T-t paths and metallogeny

L. Guillou-Frottier, . Burov, S. Cloetingh, . Le Goff, . Deschamps, B. Huet, V. Bouchot

PII: S0921-8181(11)00194-9
DOI: doi: [10.1016/j.gloplacha.2011.10.007](https://doi.org/10.1016/j.gloplacha.2011.10.007)
Reference: GLOBAL 1743

To appear in: *Global and Planetary Change*

Received date: 23 June 2011
Revised date: 12 October 2011
Accepted date: 14 October 2011



Please cite this article as: Guillou-Frottier, L., Burov, ., Cloetingh, S., Le Goff, ., Deschamps, ., Huet, B., Bouchot, V., Plume-induced dynamic instabilities near cratonic blocks: Implications for P-T-t paths and metallogeny, *Global and Planetary Change* (2011), doi: [10.1016/j.gloplacha.2011.10.007](https://doi.org/10.1016/j.gloplacha.2011.10.007)

This is a PDF file of an unedited manuscript that has been accepted for publication. As a service to our customers we are providing this early version of the manuscript. The manuscript will undergo copyediting, typesetting, and review of the resulting proof before it is published in its final form. Please note that during the production process errors may be discovered which could affect the content, and all legal disclaimers that apply to the journal pertain.

Plume-induced dynamic instabilities near cratonic blocks:
implications for P-T-t paths and metallogeny

L. Guillou-Frottier¹, E. Burov², S. Cloetingh³, E. Le Goff^{1,5}, Y. Deschamps^{1,4},
B. Huet², and V. Bouchot¹

1. BRGM, Orléans, France
2. Université P. & M. Curie, Paris, France
3. VU University, Amsterdam, The Netherlands
4. Now at : Areva, Paris, France
5. Now at: BRGM, Montpellier, France

Revised manuscript submitted to *Global & Planetary Change*
Special volume "Deep Earth"
October 12th, 2011

*: Corresponding author: Laurent Guillou-Frottier, BRGM, Service des Ressources Minérales, 3 av. C. Guillemin, BP 36009, 45060 Orléans Cedex 2, France; tel: +33 2 38 64 47 91; fax:+33 2 38 64 36 52; l.guillou-frottier@brgm.fr.

Abstract

Plume head – lithosphere interactions around cratonic blocks result in thermo-mechanical disturbances that lead to heating and burial phases of crustal rocks. We present results from numerical models of plume head - cratonic blocks interactions where a free upper surface condition and realistic rheologies are accounted for. These models include distinct cratonic blocks embedded within a continental lithosphere and separated by several hundreds of kilometres. Surface topography, thermal field and effective viscosity values are tracked for 20 Myr of interactions. The modelled dynamic interaction of a plume head around cratonic blocks results in two main types of instabilities, each of them resulting in a distinct P-T-t path. The “slab-like” instability, focused on cratonic edges when plume head is away from the craton centre, shows a near-isothermal burial phase, while the “drip-like” instability occurring above plume head material results in a near-isobaric heating phase. Consequently, both clockwise and counterclockwise P-T-t paths can be expected around cratons, as actually observed around the Tanzanian craton and other cratonic areas. Metallogenic data from gemstone-bearing rocks in south-east Africa and data from ultrahigh temperature and ultrahigh pressure metamorphism are compatible with our model. It appears that vertical mantle dynamics around cratons may also explain thermobarometric signatures that are often attributed to horizontal tectonics.

Keywords:

Cratons, mantle plumes, numerical modelling, ore deposits

1. Introduction

Thermal convection in the Earth's mantle involves large-scale horizontal motions of continental and oceanic plates at the Earth's surface. Continental drift illustrates one of the dynamic consequences of the underlying mantle convection, and subduction of oceanic plates attests to the vertical motions induced by mantle convection. In addition to horizontal and downward motions of the lithosphere, geological evidence of crustal-scale vertical motions within continents has generally been associated with horizontal tectonic forces (e.g. England and Thompson, 1984). At a larger scale, lithospheric thickening events due to horizontal shortening could trigger Rayleigh-Taylor instabilities at the base of the lithosphere (Houseman et al., 1981; Platt and England, 1994; Houseman and Molnar, 1997), and thus vertical motions of crustal rocks. Although variations in surface topography have often been related to mantle upwellings (e.g. Crough, 1978; Olson, 1990; Şengör et al., 2003), most previous studies have considered the lithosphere as a stagnant lid which surface undulations followed local isostatic compensation level. However, Gurnis et al. (2000) demonstrated how variations of dynamic topography can be used to constrain mantle density and viscosity values. Burov and Guillou-Frottier, (2005) and Guillou-Frottier et al., (2007), have later shown that due to the layered structure of the continental lithosphere, surface topography generated by plume-lithosphere interactions (PLI) may significantly differ from conventional isostatic estimations. However, vertical motions of crustal rocks resulting from PLI have not been extensively investigated.

Vertical motions of crustal rocks depend on their buoyancy and rheological behaviour and thus on thermo-mechanical constraints allowing or preventing burial and exhumation processes. At the scale of the continental lithosphere, the first order thermo-mechanical heterogeneities correspond to cratonic areas, defined by old thick rigid blocks embedded in between younger, thinner and weaker lithosphere. Burov et al. (2007) demonstrated that the craton edge, defined by a vertical thermo-mechanical contrast concentrates stresses and

strains beneath the younger lithosphere adjacent to the cratonic border. After impingement of mantle plume head at the base of the lithosphere, lateral spreading of plume head was hindered by the steep vertical craton edge while plume head spread on the other side. In this study, we examine a more common geological setting, where two cratonic blocks, separated by a few hundreds of kilometres, are inserted within a younger continental lithosphere.

When heat and mass transfer occurs in the crust, thermobarometric data provide records of possible mechanisms leading to burial and exhumation events. In a P-T diagram where pressure increases upwards, a clockwise P-T-t path describes a burial phase during which the peak pressure precedes the peak temperature, thus leading to a near-isobaric heating phase. In contrast, a counterclockwise P-T-t path shows that the peak temperature is reached before the peak pressure, defining a near-isothermal burial phase. In terms of source mechanisms, fast subduction can explain clockwise P-T-t paths (i.e. fast burial episode; e.g. Agard et al., 2009), while mantle underplating may give rise to counterclockwise P-T-t paths (e.g. Warren and Ellis, 1996). Within granulite terrains, the coexistence of clockwise and counterclockwise P-T-t paths has been explained by different conflicting models calling for either slab rollback or significant mantle upwelling (e.g. Collins, 2002; Brown, 2001; Collins 2003). Recent analysis of ultra-high temperature (UHT) metamorphism in mafic granulites from southern India revealed the important role of heat input from the mantle (Prakash et al., 2010). For thrusting events, both patterns may also coexist depending on burial and erosion rates, and initial thermal structure (e.g. Ruppel and Hodges, 1994).

Following up on numerous studies of the effects of tectonic stacking or downward subduction on P-T-t paths, we investigate the impact of mantle upwellings on thermo-mechanical processes affecting crustal rocks around cratonic areas. Our approach is partly motivated by the spatial distribution of distinct types of ore deposits in east Africa, near the Tanzanian craton. In addition, an apparent asymmetrical behaviour seems to occur between one side of the craton and the other, as recently suggested by geochemical signatures of erupted lavas (Chakrabarti et al., 2009). In this context, geological, thermobarometric and

metallogenic data around cratonic areas, and in particular around the Tanzanian craton, are compared with the modelling results.

2. Mantle plumes beneath cratons

The presence of continents, their sizes, and their distribution at the Earth's surface strongly controls the dynamic regime of the mantle. It has been demonstrated that plate velocities, convective wavelengths, and mantle temperatures are to a large extent affected by the heterogeneous character of the Earth's surface (Elder, 1967; Hewitt et al., 1980; Guillou and Jaupart, 1995; Trubitsyn et al., 2003; Lenardic et al., 2005; Coltice et al., 2007; Phillips and Coltice, 2010). From the Earth's mantle, the upper thermal boundary condition is heterogeneous (presence of oceans and continents) and depends, for example, on the amount of continental masses, whose spatial distribution varied through geological time history. Laboratory experiments by Guillou and Jaupart (1995), where a heterogeneous thermal condition at the top surface mimicked the presence of a continent, showed that within the convecting fluid, a vertical upwelling of deep hot material was always locked beneath the central part of the "continent". Since Archean cratonic zones are generally surrounded by Proterozoic belts, they can be considered as inner parts of continents, from which underlying mantle flow tend to diverge, thus facilitating the arrival of an underlying thermal plume.

Upwelling currents of hot and deep mantle material (here referred to "mantle plumes") stand for perturbations acting on the lithosphere that could lead to various deformation modes (e.g. Burov and Cloetingh, 2009). Numerous studies suggest that several tens of mantle plumes are present in the current convective pattern of the Earth's mantle (e.g. Jellinek and Manga, 2004; Montelli et al., 2004). In the present-day Earth, seismic tomography has revealed anomalously hot zones hundreds of kilometers wide (Zhao, 2004; Koulakov et al., 2009). Depending on their size, various types of upwelling plumes have been described, from "baby-plumes" beneath western Europe (e.g. Ritter et al., 2001) to "superplume" events in the past (Condie, 2002) or present-day "mega-plumes" in the lower

mantle, such as large-scale upwellings beneath Africa and Pacific (Forte and Mitrovica, 2001; Romanowicz and Gung, 2002; Dziewonski et al., 2010). Successive formations and destructions of supercontinents have probably induced several episodes of large-scale thermal blanketing and consequent superplume (or plume clusters) events. Therefore, through the Earth's history, cratonic roots of continents which were either isolated or embedded within a supercontinent were probably pounded by heads of small and large-scale mantle plumes. This scenario stands for the basic hypothesis of our study, where mantle plumes regularly impinged on the base of cratons. In section 3, numerical experiments show details about a single plume-craton interaction, on a short time scale of 20-30 Myr, but dynamic consequences are here supposed to occur regularly through several episodes of plume head – cratonic block interactions.

Present-day active interaction between mantle convection and continental lithosphere probably occurs in east Africa, where surface tectonics and volcanism around the Tanzanian craton illustrate the role of cratonic zones. Recent research focused on this area showed spatial distribution of the structural features related to craton-mantle interactions, emphasizing the crucial role of the Archean craton stiffness when compared to the weak adjacent Proterozoic belts (Ebinger et al., 1997; Petit and Ebinger, 2000; Corti et al., 2007). Tectonic inheritance, differences in rheological properties, but also location of lithospheric weakness zones can explain spatial organisation of continental rifts around the Tanzanian craton. It is likely that concentration of shear zones and location of rift structures around the stiff craton also promotes vertical motions of crustal rocks whereas stabilized cratonic zones are not expected to record such thermo-mechanical disturbances. Surface topography, which presumably reflects underlying vertical motions of crustal rocks, appears to be significantly affected at cratonic margins, whereas flat topographic signatures are observed above cratons (e.g. Burov and Guillou-Frottier, 2005; Wallner and Schmeling, 2010). However, dynamic signatures also depend on rheological properties of the continental lithosphere, and it is thus important to investigate distinct thermo-mechanical regimes of the lithosphere when it is impinged by a mantle plume.

The fate of plume heads impinging on the base of - or near - cratonic roots has been the subject of several scenarios, from ponding of mantle material beneath cratons (e.g. Silver et al., 2006) to lateral flow towards the craton edges (e.g. Ebinger and Sleep, 1998). In addition, there is growing evidence that removal of lower lithosphere occurred around cratonic blocks in the past (e.g. North China craton, Gao et al., 2008). Ultrahigh temperature metamorphism occurs near cratonic margins (see Kelsey, 2008 for a review) and contrasting (clockwise and anticlockwise) P-T-t paths have been detected in the vicinity of cratonic areas (e.g. east Antarctica, Halpin et al., 2007).

Amongst the numerical models simulating plume head - cratonic block interactions, few incorporate realistic formulations for the lithosphere and the mantle. For example, most models use a rigid boundary on the top of the model (see, however, Pysklywec and Shahnas, 2003; Lenardic et al., 2003), i.e. the upper surface is not deformable (e.g. Trubitsyn et al., 2003; van Thienen et al., 2003). In addition, lithosphere and mantle rheologies are often too simplified for adequate studies on plume-lithosphere interactions: constant viscosities for the lithospheric mantle (Pysklywec and Shahnas, 2003) or Newtonian laws (Elkins-Tanton, 2007) implicitly ignore the rheological stratification of the lithosphere. An important objective of this study is, therefore, to explore possible convective instabilities around cratonic blocks with a thermo-mechanically coupled numerical approach that has been previously used to model mantle-lithosphere interactions for scenarios invoking a laterally homogeneous lithosphere (d'Acremont et al., 2003; Burov and Guillou-Frottier, 2005) or a single lateral heterogeneity (Burov et al., 2007), as illustrated in Figure 1. Modeling results presented here centre on lithospheric instabilities occurring near cratonic margins, and their consequences for the dynamic topography and associated P-T-t paths.

3. Numerical models

3.1 Basic approach

The need for including lateral heterogeneities in models of plume head – continental lithosphere interactions has been demonstrated in previous studies (Burov et al., 2007), which were limited to the influence of one cratonic margin. Main differences between other previous numerical modelling studies and our thermo-mechanical modelling approach are in the account of (i) a free upper surface condition; (ii) an explicit elastic-viscous-plastic rheology; and (iii) a stratified structure of continental lithosphere (see details in Burov and Guillou-Frottier, 2005 and in the electronic supplementary material). In contrast to convective models that are commonly adopted to study mantle-lithosphere interactions, our model permits to investigate the transient evolution of dynamic topography and of deep (lithospheric) dynamical instabilities resulting from rheological changes induced by plume-cratons interactions. In addition, the implementation of particle-in-cell technique combined with a consistent account for pressure (solution of motion equations for full stress tensor instead of that for shear stress tensor as in most convection models) allows us to trace P-T-t paths of selected particles and compare them with thermobarometric data. For the sake of simplicity, we used Boussinesq approximation for density. Yet we also made some tests accounting for density variations due to full-scale phase changes through PERPLEX (Conolly, 2005; Burov and Cloetingh, 2009, see also supplementary material). Comparisons with the results based on conventional (constant thermal expansion coefficient) Boussinesq approximation, revealed some differences (see also Burov and Cloetingh, 2009) that do not, however affect the behavior of the system as a whole in the context of the present study.

The majority of previous studies have not addressed the most common geological configurations, where two or more cratonic blocks with a small size are separated by areas of dimensions of hundreds to a few thousands of kilometres-long younger continental crust. Examples can be found in several areas (see the map of present-day Archean cratons by Kusky and Polat, 1999), including the Yilgarn-Pilbara Archean (Australia), Guyana-Sao Francisco (South America), Slave-Hearne (North America), Aldan-Anabar (Siberia), Zimbabwe-Kaapvaal (South Africa), and Tanzanian-Madagascar blocks (East Africa).

3.2 Model setup and description of the experiments

The numerical model and its applications were described in previous studies (Burov and Molnar, 1998; Burov et al., 2003; d'Acremont et al., 2003; Burov and Guillou-Frottier, 2005; Burov et al., 2007; Burov and Cloetingh, 2009, see also supplementary electronic material). Below, we therefore limit ourselves to specific features of the new numerical experiments.

The numerical box is vertically limited to the upper mantle (650 km depth) and has horizontal dimension of 1500 km (Figure 1). The initial plume diameter (spherical density contrast associated with 150°C temperature difference) has a diameter of 100-200 km (200 km if not mentioned otherwise) and is located at the centre of the bottom boundary, except in the first experiments where only one cratonic margin is present (Burov et al., 2007). Apart from this case, the continental lithosphere comprises two 300 km-long and 150 km-thick "cratonic" (actually simply older) blocks, or terrains, separated by a younger continental belt, 100 km-thick in reference case, 300 km large. Although the dimensions of the blocks at first sight may appear small, the presence of a lateral heterogeneity is more important than the width of the heterogeneity itself (Burov et al., 2007; Burov and Cloetingh, 2009). Here, the chosen distance between the two cratons allows to examine the case where a plume head could be locked in between the two thick blocks, reflecting the typical configuration encountered in African continent. The thickness of the non-cratonic continental lithosphere that surrounds the blocks has been varied from the cold thick case (200 km) to a thin weak case (100 km). In Figures 1a-1c, black, grey and white stripes illustrate rheological layering of the lithosphere. The chosen rheological laws and initial temperature profiles are shown in Figure 1d (see caption and details in Table 2). Thermal and mechanical boundary conditions are detailed in caption of Figure 1. The "cratonic" blocks have the same thermo-mechanical structure as in Burov et al. (2007) with a thickness of 50 km in excess of the thickness of the surrounding lithosphere. To investigate the role of distinct convective regimes, low (10^5) and high (10^7) plume Rayleigh number experiments have been performed. The plume Rayleigh

number is defined in Burov and Guillou-Frottier (2005) and use maximal driving density contrast and effective viscosity (see supplementary material, A4).

3.3 One lateral heterogeneity

The results shown in Figure 2 illustrate the predictions from models involving a single lateral heterogeneity (see also Burov et al., 2007). For each case, the craton (800 Ma age) is embedded within a thin weak lithosphere (150 Ma age). These models show the development of three distinct lithospheric downwellings leading to the burial of mantle lithosphere. These downwellings are thermally revealed by distinct geometries. In the first case where the plume is initiated below the thick craton (dotted semi-circle, Figure 2a), return flow from the left edge of plume head entrains a large amount of lithosphere (blue zones in the phase field) within the mantle. When the plume starts below the lateral heterogeneity (Figure 2b), a "drip-like" instability, labelled "2" in the thermal field, occurs at shallow depths after plume head material has softened the lower crust. This instability occurs at a certain distance of the cratonic boundary since the plume head centre is laterally deviated towards the thin lithosphere. When the plume starts below the thin lithosphere, at a certain distance from the cratonic edge (Figure 2c), plume head spreading is still hindered by the vertical cratonic margin, but the return flow around plume edges affects the cratonic root margin and mechanically entrained part of it downwards (see the green-yellow area labelled "3", sinking into the mantle). This "slab-like" instability is also incipient in the previous case, but appears to be more efficiently initiated when plume starts away from beneath the cratonic margin.

Delamination of the mantle lithosphere by drip-like instabilities, resulting in compressive stresses at the surface, as well as topographic signatures of plume – lithosphere interactions, are useful results to interpret geological processes explaining structural and geochemical records of the Columbia River flood basalts (Camp and Hanan, 2008). In particular, compressive zones at cratonic edges (see circular diagrams in Figure 2) correspond to the highest topography gradient (2000-3000m of elevation difference over less

than 100 km), whereas extensive zones show only small-amplitude and short-wavelength topographic variations.

Temporal variations of topography correspond, at depth, to burial and exhumation processes. The right column of Figure 2 suggests contrasting P-T-t paths followed by crustal material buried by the three distinct downwellings. Crustal material can be heated up to 1000-1200°C before being buried (instabilities 1 and 2), or can be pushed downward at temperatures below 900°C by plume edges before being heated (instability 3, slab-like). The consequent P-T-t paths illustrate both clockwise and anticlockwise trajectories. These P-T-t trajectories being obtained qualitatively, a more rigorous investigation (numerically deduced) in the case of two cratonic blocks is presented in section 3.5.

3.4 Results with two cratonic blocks

3.4.1. Thick continental lithosphere. Figure 3 shows four snapshots of the ascent of a mantle plume beneath a 200 km-thick strong continental lithosphere, where two 250 km-thick cold blocks are embedded. The rheological stratification of the lithosphere is reflected in the middle column (effective viscosity) where the ductile lower crust is outlined in non-cratonic areas (yellow region between the strong upper crust and the upper mantle), and where thick and cold blocks can be mechanically defined by a stiff cratonic keel. 1.5 Myr after plume initiation, the plume head has already reached the base of the lithosphere, between the two cratonic blocks. The plume head spreading phase is symmetric (see thermal field) and plume material erodes the base of the lithosphere (see the effective viscosity column), resulting in a smoother topography at the base of cratons. Surface topography reacts as if the crust was mechanically coupled to the lithospheric mantle since a single large-scale uplift is observed. It can be noted that at the final stage (16 Myr) two (small) drip-like instabilities are incipient at the base of the central part of the lithosphere (see the temperature field).

This numerical experiment demonstrates that the thermo-mechanical stability of a thick strong lithosphere is not affected by plume head dynamics, although small-scale drip-like instabilities can be triggered at the base of the lithosphere.

3.4.2 *Thin continental lithosphere*. This case has been investigated for two distinct dynamical regimes of the mantle, described by low and high plume Rayleigh numbers (Ra_p).

At low Ra_p (Figure 4a), the head of the large-scale plume entrains shallow mantle material down to the plume sides, implying a whole negative subsidence of the lithosphere. After a gentle negative deflection at 2.4 Myr, subsidence at locations between the two cratonic blocks is accelerated yielding a 2000m topographic low. Due to the presence of stiffer - and thus less deformable - cratonic blocks, subsidence is focused and restricted to this weak internal zone (called "crumple zone" by Lenardic et al., 2003), much more deformable than the surrounding cratons.

Figure 4b is a close-up of this area at time 15 Myr, and shows lateral segmentation of crustal rheology (i.e. lateral variations of the effective viscosity), thus promoting crustal-scale deformation. During the experiment, topographic uplift above cratonic areas continuously increases. At time 15 Myr, topographic plateaus of more than 1000m are formed above cratonic areas. The large plume head brings up large quantities of hot mantle material, leading to a more efficient thermo-mechanical erosion of the thin part of the lithosphere. At the surface, alternating zones of extension and compression result from plume head penetration within the mantle lithosphere. The phase field at that time clearly illustrates that thermo-mechanical erosion of the lithosphere results in the entrainment of non-lithospheric mantle material near the base of the crust (Figure 4b).

Figure 5a to 5c show experiments characterized by high $Ra_p \sim 10^6$, based on thermodynamically consistent computations. For that we have coupled the thermomechanical code with the thermodynamic model PERPLEX (Connolly, 2005; see Appendix A3). This allows for computation of mineralogically and thermo-dynamically consistent densities and elastic parameters of rocks that are directly updated during the thermo-mechanical computations (see Burov and Cloetingh, 2009). Figure 5a shows that for the same initial plume diameter as in the previous case (low Ra_p), the plume head rises faster. In contrast with the previous case, the central zone embedded between cratons undergoes a significant uplift (Figure 5a, bottom right). With time, the stiffer cratonic blocks

are progressively uplifted while the central zone subsides (time 15 Myr; Figure 5a). The plume head spreading is slowed down by the cratonic roots. The phase field shows that plume head is split in two parts which dynamically support the cratonic blocks and maintain the topography above the cratons. As shown in the thermal field, heating of the lithospheric mantle induces Rayleigh-Taylor-like instabilities at plume head centre and beneath cratons. At time > 3 Myr, small-scale “slab” or “blob” –like instabilities are observed at the very edges of plume head, at both cratonic edges (see burial of cratonic material in the phase field). At that time, the plume head has only begun its flattening stage and lateral heterogeneities are entrained downwards. The flattening stage then prevents subduction of subcontinental lithospheric mantle to proceed further (time step of 15 Myr). On the base of experiments with a single heterogeneity (Burov et al., 2007) it can be predicted that in the case when two cratonic blocks are separated by a distance greater than the plume head diameter, the lateral edge of craton will hinder plume head flattening, promoting development of slab or blob-like instabilities and shear stresses concentration at cratonic margins.

For comparison, Figure 5b shows an experiment where cratonic blocks are only slightly thicker (only 25 km) than the embedding lithosphere. In this case plume spreading is not hindered and plume head removes almost all mantle lithosphere in less than 12 Myr. This experiment highlights the importance of the cratonic blocks, and lateral lithospheric heterogeneities in general, as localizing factors for plume-related deformation. Finally, a “cold” experiment shown in Figure 5c demonstrates plume-lithosphere interaction in case of colder background geotherm in the upper mantle (1750°C at 650 depth). This condition corresponds to the hypothesis of whole mantle convection (Schubert et al., 2001). As can be seen, the assumption of a colder background geotherm does not mitigate the consequences of plume impact (see also discussion in Burov and Cloetingh, 2009).

3.5 P-T-t paths around cratonic margins affected by mantle plumes.

Figure 6 shows a series of retrograde P-T-t paths deduced from the simulation shown in Figure 5. The followed particles are located near the inner cratonic margins where Rayleigh-

Taylor like instabilities develop (see black dots in Figure 5a). For the deeper lithospheric material ascending towards the surface (path number 1), the clockwise P-T-t path includes a near-isothermal decompression phase around 800-900°C. For material coming from Moho depths (paths number 2), the clockwise P-T-t paths exhibit near-isothermal decompression episodes at lower temperatures (~ 700-750°C). However, for material coming from middle crust, the four particles follow anti-clockwise P-T-t paths with maximum (P,T) values reaching 920°C and 1.3 GPa (green dashed-dotted lines).

P-T-t paths shown in Figure 6 represent 20-30 Myr of metamorphic evolution. The slow cooling phases identified in paths number 2 (blue and orange plain lines, from maximum temperatures around 700°C to depths of 0.4 GPa where $T=650^{\circ}\text{C}$) are equivalent to cooling rates of about 5-9°C/Ma.

It is noteworthy that paths number 2 reach almost zero pressure levels, that some would interpret as exhumation to the surface, whereas the corresponding phase field in Figure 5 does not always reveal exposure of initially buried lower crustal units to the surface (pink layer in Figure 5a). This is because the grid elements have dimensions of 5x5 km; their colors in Figure 5a correspond to an average dominant phase in the element, while the isolated particles (markers) used for PT tracing may be several km above the center of the mass of the element. In the model, there are about 20 phase markers per grid element yielding sub-grid resolution on the order of 1x1 km. On the other hand, the main grid resolution of 5 km implies that pressure, referred to the centers of the cells, is resolved with accuracy on the order of 75 MPa (150 MPa change over the cell). Extension at the surface creates dynamic (tectonic) pressure on the order 20-100 MPa, involving that conversion of pressure to depth may have an uncertainty on the order of 1-2 km at shallow depths, 5 km between 10 and 20 km depths, and 10-15 km below 20 km depth (Figure 8). This circumstance is specific for the lithosphere, since its high strength can support important non-lithostatic pressures. This issue has been previously discussed by Petrini and Podladchikov (2000). It is noteworthy that such pressure-depth conversion ambiguities are specific to the areas of non-localized deformation. For example, P-T-t paths from faults and

subduction channels are likely to be lithostatic, while in other cases important deviations may be expected. In any case, such deviations do not exceed 5-10% of the maximum values shown in Figure 6.

4. Mineral resources near cratonic margins

Most studies dealing with mantle plumes and mineral resources signatures around Archean cratons were focused on diamond genesis and kimberlitic eruptions (e.g. England and Houseman, 1984). The recent study by O'Neill et al. (2005) emphasizes the role of intracontinental heterogeneities where abrupt changes in lithospheric thickness occur, promoting favorable conditions for diamond exhumation. Our study accounts for additional metallogenic data including gemstones and plutonic-related tin (Sn ± W-Ta-Li-Be) deposits (e.g. Milesi et al., 2004). Relationships between gemstones, cratons and mantle plumes are briefly presented below and specific data from east Africa are presented in section 5.

4.1 Gemstones

The formation and the exhumation of metamorphic gemstones require distinct geodynamic processes occurring at high pressures and high temperatures, thus involving the dynamics of the lithospheric mantle. Diamonds are stable at depths greater than 180 km (Boyd et al., 1985), and can thus remain stagnant beneath the thickest parts of Archean cratons, until kimberlitic explosive volcanism induces their fast exhumation. Other gemstones such as rubies and sapphires derived from metamorphic and metamorphic-metasomatic processes, have also recorded high-pressure and high-temperature conditions (typically between 650 and 800°C and between 0.6 and 1GPa) at the time of their formation (e.g. Sutherland et al., 1998; Shaw and Arima, 1998; Santosh and Collins, 2003; Simonet et al., 2004) but contrary to diamonds, they are mainly found at cratonic margins or within the neighbouring Proterozoic mobile belts (Le Goff et al., 2004; Giuliani et al., 2007; Le Goff et al., 2010). Rubies and sapphires associated with magmatic processes are often related to mafic-

alkaline rocks (e.g. Yui et al., 2003) and gem-bearing basaltic volcanism has already been suggested to derive from a mantle plume activity (Sutherland and Fanning, 2001).

4.2 Other rocks and ore deposits

A number of authors have advocated mantle plume events to explain geological and metallogenic features related to cratonic areas. For example, in Precambrian times, several superplume events have been suggested to account for apparent pulses of continental growth and metallogenic crises (e.g. Condie, 2002; Pirajno, 2004). Reconstructions of paleo-supercontinents through the Earth's history suggest that major metallogenic crises occurred during periods of superplume activity leading to breakup of supercontinents (Teixeira et al., 2007). In addition, world-class Ni-Cu-PGE ore deposits have been proposed to be related to ultramafic volcanism derived from mantle plumes and located on the edges of cratonic blocks (e.g. Arndt et al., 1997; Zhang et al., 2008).

At first sight it was expected that plume head - continental lithosphere interactions would result in uplift phases and melting episodes. However, so far these signatures have been usually interpreted in terms of other tectonic processes, and only occasionally, mantle upwelling has been suggested as a possible source for burial of lower crustal material (Saleeby et al., 2003; Smithies et al. 2003). The presence of eclogites is often associated with the oceanic subduction process, and some authors used eclogites as evidence of past subduction (Möller et al., 1995). However, as suggested by our experiments, eclogites could have formed through interaction of a mantle upwelling and the consequent downward dynamic instability. The latter conceptual model is corroborated by P-T-t data recorded on mineral assemblages from rocks of east Antarctica, that show both clockwise and counterclockwise P-T-t paths from rocks located near cratonic margins. To resolve this paradox, Halpin et al. (2007) have proposed a complex scenario involving two apparently opposite dynamic processes. Namely, records of both clockwise and counterclockwise P-T-t paths would suggest that two distinct exhumation histories could coexist near cratonic

margins. However, our numerical experiments suggest that these observations can also be explained with a single mantle-lithosphere interaction model.

5. Signatures of plume-cratons interactions in East Africa

5.1 Recurrent plume activity

According to recent seismic tomography studies (Ritsema et al., 1998; Weeraratne et al., 2003; Walker et al., 2004; Montagner et al., 2007), the Tanzanian craton is probably at least 150 km thick with a surrounding asymmetric mantle flow. The present-day plume head which would be present under the lithospheric keel corresponds to a 200-400 km wide thermal anomaly (Nyblade et al., 2000). It should also be noted that numerous episodes of rifting-related magmatism have been inferred for the past geological evolution around Tanzania. In particular, the east African rift area has been affected by at least four alkaline-peralkaline magmatic and carbonatitic events, beginning at the end of the Mesoproterozoic (around 1 Ga, Meponda in Mozambique and Ngualla in Tanzania), and subsequently continuing in successive spurts with displacement of the magmatic centres in the Neoproterozoic around 730-655 Ma (Lueshe district), in the Early Paleozoic (Lueshe, Matongo), and then in the Late Jurassic - Late Cretaceous in the southern segment of the rift (Panda Hill in Tanzania, Kangankunde-Nathace in Malawi) (Milesi et al., 2004; Milesi et al., 2006; Le Goff et al., 2010). This heterogeneity and the distribution of alkaline-peralkaline plutonic activity around organized centres, suggest the operation of mantle plumes at four different periods (Pouradier, 2002), spanning at least 1 Ga. One recent study also concludes that the intracratonic Congo basin reveals a hidden rift structure which was periodically affected and weakened during a long period of time (Kabongo et al., 2011)

5.2 Diamonds

As well known, a striking correlation appears between primary diamond deposits and Archean cratons. It is now commonly accepted that the P-T conditions for stability field of diamond implies that they are stored beneath thick (>150-180 km) Archean cratons. Figure 7

(top row) shows primary diamond deposits of south and east Africa together with contours of Archean cratons. Diamonds of south and east Africa have formed at 3.2, 2.9, 1.5 Ga, and were exhumed through kimberlitic magmatism at three main periods in the last 1150 Ma (Richardson et al., 2004).

5.3 Other gemstones

The famous "Gemstone belt of East Africa" (Malisa and Muhongo, 1990) is located in between Tanzanian and Madagascar cratonic areas, i.e. within the Neoproterozoic Mozambique belt. It includes numerous gemstone deposits yielding ruby, sapphire, garnet, tourmaline and various other gems (Simonet, 2000). Contrary to diamonds, formation of syn-metamorphic gemstones occurs at depths of a few tens of kilometers, and their exhumation does not require explosive eruptions, except in the case of the so-called "basaltic sapphires" related to the Neogene alkaline rift volcanism. Thermobarometric data from ruby-bearing rocks from Madagascar and Kenya indicate that P-T conditions of ~ 1 GPa and 800°C were reached (Mercier et al., 1999a, 1999b). According to several other studies, the stability field for corundum-quartz and corundum-garnet-clinopyroxene assemblages in other ruby-bearing rocks involve more extreme P-T conditions, such as $P > 1.5$ GPa and $T > 1100^\circ\text{C}$ (Shaw and Arima, 1998; Rakotondrazafy et al., 2006; Schenk et al., 2004).

Figure 7 (bottom left) illustrates the spatial distribution of ruby and sapphire deposits around cratonic areas. The high P-T conditions which are required for their formation are reached between cratonic areas, but surprisingly, the distribution is not symmetric. Actually, no gemstone deposit appears on the western side of the Tanzanian craton. The continuity of the gemstone belt from Kenya to south Madagascar confirms that this particular inter-cratonic area underwent severe burial and exhumation processes, contrary to the western part of Tanzania.

5.4 Tin

The bottom right of Figure 7 shows the spatial distribution of felsic intrusion-related tin deposits (Sn ± W, Ta, Li, Be). Classically, felsic intrusion-related tin concentrations derive from pneumatolitic (late-magmatic) tin-bearing fluids (400-600°C) related to specialized (peraluminous) felsic magmas. Focused outside cratonic areas, the numerous tin districts evidence periods of crustal melting, in particular within the Mesoproterozoic Kibaran orogenic belt produced by the collision of the Congo and Tanzanian cratons. The Mesoproterozoic cycle concluded around 1000-950 Ma with a plutonic to volcano-plutonic event, and with the emplacement of gneissic complexes in the internal domain. This Lurian late-orogenic crustal magmatic event, distinguished by a peraluminous signature, is expressed by numerous tin-tantalum granites and pegmatites in Rwanda, Burundi, southern Uganda, western Tanzania, Kivu and Maniema, eastern Congo (Milesi et al., 2004; Milesi et al., 2006).

The notion that no tin deposits are found within cratons is not surprising since crustal melting can be induced by post-tectonic events or by heat input at crustal depths, two scenarios which can be ruled out in a tectonically stable and thick cratonic area. Nevertheless, the absence of intrusion-related tin deposits at the eastern side of the Tanzanian craton area suggests that either crustal melting in this area was quantitatively limited, or that another type of dynamic interaction between the mantle and the lithosphere occurred.

5.5 Eclogites and granulites

A series of additional thermobarometric data demonstrate that extreme P-T conditions were present near the Tanzanian craton borders. Among them, the Paleoproterozoic (2.0 Ga) eclogites found at both south-east and south-west margins of the craton (Usagaran and Ubendian belts, respectively) indicate an exhumation process starting with conditions of ~1.8 GPa and 700°C and following a clockwise P-T-t path (Möller et al., 1995; Collins et al., 2004). In addition, metagabbros from the Ubendian terrane were also affected by metamorphic conditions of about 840-900°C and pressures of 1.2-1.4 GPa (Muhungo et al., 2002).

During the Paleoproterozoic orogenic cycle, high temperature metamorphism (850-900°C; 0.8 GPa) occurred in the southern margin of the Tanzanian craton (Schenk et al., 2004). On the other side (northern margin), ultrahigh temperature metamorphism (~1000°C and 0.7-0.9 GPa) has been recognized in Labwor hills, Uganda (Sandiford et al., 1987).

Close to the eastern margin of the Tanzanian craton, Neoproterozoic metamorphism of high pressure granulite facies was reported (Muhongo and Tuisku, 1996; Appel et al., 1998; Möller et al., 2000; Cutten et al., 2006; Sommer et al., 2008). Thermobarometric results and isotopic dating revealed anticlockwise P-T-t paths, where conditions of peak metamorphism give a pressure range between 0.9 and 1.2 GPa at 800°C. However, a recent analysis by Sommer et al. (2008) reveal clockwise P-T-t paths (with an isothermal decompression phase) for the "Western Granulite" terrane, with P-T conditions of 1.3-1.4 GPa and 760-800°C.

5.6 Summary of geological observations

Figure 8 summarizes the above described thermobarometric data from the Tanzanian area. Estimates of P-T data and inferred P-T-t paths suggest that burial and exhumation episodes probably occurred through distinct processes, since clockwise and anti-clockwise P-T-t paths are both recorded.

The asymmetry in geological signatures around Tanzania (e.g. location of gemstone and tin deposits, contrasting P-T-t paths) points to distinct thermo-mechanical mechanisms at both sides of the craton. Even if gemstones and tin deposits are not coeval, the comparison can be considered valid since the craton is supposed to have undergone a similar thermal history through more than 1 Gyr: successive mantle plumes have probably followed similar mantle paths before impinging on the base of the craton.

6. Discussion

Models of plume head – cratonic blocks interactions have shown that contrasting P-T-t paths can be retrieved from rocks at cratonic margins initially emplaced at different depths (Figure 6). General shapes of numerical P-T-t paths (clockwise and counterclockwise paths), absolute values of pressure and temperature, as well as cooling rates can be quantitatively compared to thermobarometric data recorded around the Tanzanian craton. In addition, thermo-mechanical instabilities induced by plume head – cratonic block interactions show two distinct processes leading either to isobaric heating before burial (the “drip-like” instability) or to isothermal burial before heating (the “slab-like” instability). Drip-like instabilities would trigger counterclockwise P-T-t paths whereas slab-like instabilities would promote clockwise P-T-t paths. In addition to these modelling results, distribution of geological and metallogenical signatures in east Africa suggests that distinct deep processes occurred and still occur on both sides of cratonic areas.

Previous hypotheses to account for the observed variety of P-T-t paths were generally associated with horizontal tectonics and downward motions induced by subduction dynamics. Our modelling study suggests mantle upwellings as a driving mechanism for crustal metamorphism.

The subcontinental mantle upwelling may represent the missing heat source that seems to be required when ultra-high temperature metamorphism is investigated. For example, Schmitz and Bowring (2003) suggested transient removal of lithospheric mantle to explain thermobarometric data showing UHT metamorphism around the Kaapvaal craton, south Africa. Similarly, Prakash et al. (2010) invoked accretion of mantle-derived magma to explain the additional heating required by P-T data around the Dharwar craton. Besides providing the necessary heat input, drip-like instabilities would also represent an efficient mechanism to remove the lithospheric mantle and replace it by mantle-derived magmas. It must be noted that such deep processes involving lithospheric instabilities have already been invoked to explain particular strain patterns identified around the Dharwar craton (Bouhallier et al., 1995; Chardon et al., 1998). Archean and Proterozoic tectonics might have been

significantly affected - if not controlled - by Rayleigh-Taylor like instabilities which easily occurred at cratonic boundaries beneath hot and weak lithospheres.

As far as ultra-high pressure metamorphism (UHP) is concerned, most models invoke continental subduction to explain nearly isothermal burial down to depths of 80-100 km (e.g. Brown, 2001). Here again, edges of mantle plume heads can mechanically entrain mantle lithosphere down to several hundreds of kilometres, while temperature does not necessarily increase much. The resulting clockwise P-T-t path shows peak pressures in excess of 1 GPa (Figure 6). As for subduction-triggered burial of crustal rocks, the subsequent exhumation process would then be driven by buoyancy forces.

Figure 9 illustrates the basic concepts developed in this study: (a) a large cratonic area attracts and focus the arrival of a large-scale mantle upwelling, resulting in continental breakup into smaller cratonic blocks, as it was probably the case for the Tanzania-Madagascar-Dharwar continental aggregation; (b) smaller mantle plumes continue to impinge at – or near - the base of cratonic blocks; (c) when mantle plumes rise beneath the Tanzanian craton, heads are deflected westwards because of a sloping basal topography (e.g. Sleep et al., 2002), thus inducing (d, left) drip-like instabilities, counterclockwise P-T-t paths, and partial melting of the lower crust; ultrahigh temperature metamorphism is also promoted and granite-related ore deposits can form; (d, right) when mantle plumes rise beneath the eastern side of the Tanzanian craton, plume heads are blocked by the vertical cratonic edge, favouring slab-like instabilities, clockwise P-T-t paths and ultrahigh pressure metamorphism, as well as formation of gemstones or eclogites. Such mechanisms inferred from numerical simulations of plume head – cratonic block interactions exhibit metamorphic signatures very similar and with the same amplitudes as those recorded around cratonic margins.

Acknowledgements. This study was partly supported by BRGM, UPMC and ISES. We thank F. Neubauer, R. Oberhänsli and previous anonymous reviewers including P. Rey for helpful comments that greatly improved the final version of this paper.

ACCEPTED MANUSCRIPT

Figure captions

Figure 1: Numerical set-up of plume- continental lithosphere interactions: a) case of a homogeneous lithosphere (see Burov and Guillou-Frottier, 2005) with no pre-imposed horizontal velocity at horizontally “permeable” (see Burov and Cloetigh, 2009) vertical boundaries (arrows); a free surface condition and hydrostatic pressure are imposed at the top and bottom boundaries, respectively; vertical boundaries are thermally insulating (zero outflux) while fixed temperatures of 0°C and 1750°C (whole mantle convection) or 2000°C (double-layer convection) are imposed at top and bottom boundaries, respectively; b) case of a lateral intraplate heterogeneity (see also Burov et al., 2007) with identical thermo-mechanical boundary settings; c) this study, where two cratonic blocks are present with identical thermo-mechanical boundary settings; d) initial thermo-mechanical conditions for lithosphere and cratonic crust are indicated in the three diagrams. When not stated otherwise, we assumed double-layer convection geotherm for the upper mantle below the lithosphere. Lithospheric geotherms are shown for different thermotectonic ages (left); corresponding yield strength are computed for a constant strain rate of 10^{-15} s^{-1} (middle); initial mantle geotherm (right). The thermo-mechanical regime of the lithosphere approaches steady-state starting from 400 Ma age (see Burov et al., 2007 for additional details).

Figure 2: Experiments for a case with a single lithosphere heterogeneity for three distinct initial plume locations (dotted half-circle). A 800 Myr old craton is inserted in the half-right part of the 150 Myr old lithosphere (dotted line shows the initial configuration). From top to bottom, time steps correspond to 7.2 Myrs, 11.3 Myrs, and 16.5 Myrs. Color code for the phase field (left column): purple: crust, blue: mantle lithosphere, green: upper mantle, yellow: plume, orange: marker layer at the bottom. Note the three kinds of lithospheric instabilities (black arrows and white numbers): 1: subduction-like instability (a), 2: drip-like instability (b) and 3: slab-like instability (c). Third column illustrates three qualitative distinct P-T-t paths followed by associated instabilities, as inferred from the temperature field in the second column. Based on Burov et al. (2007).

Figure 3 Case of a thick (200 km) lithosphere with two cold blocks. Temperature in °C, log (effective viscosity) in Pa.s, and surface topography in m. Note that surface topography consists mainly in one

single domal signature (see text). At time step 16 Myr, two incipient drip-like instabilities are visible in the thermal field.

Figure 4: a) Low (10^5) plume Rayleigh number experiment, with two cratonic blocks and a thin weak lithosphere. The low plume Rayleigh number promotes the formation of a large plume head with a large plume tail. The large-scale return flow induces a negative topographic signature (i.e. subsidence) above the plume head. At the final stage, alternating zones of extension and compression are present between cratonic areas; b) Close-up of the last time step, where thermo-mechanical interactions between the plume head and the non-cratonic lithosphere imply a lateral segmentation of crustal rheology.

Figure 5: Thermodynamically consistent model (density computed from PERPLEX (see A3) as function of P and T), where the resulting Rayleigh number is high ($\sim 10^6$) Here, the colour code for the continental crust is different for the upper crust (red-orange) and the lower crust (pink). a) Topography reacts positively (localized uplift) at the inner borders of the blocks, whereas negative signatures progressively develop around cratonic margins and within the intermediate young lithosphere. Note incipient drip-like instabilities and small-scale upwellings at 15 Myr and later stages (temperature field). At 15 Myr, rotating movements (up and down instabilities) in the lithosphere mantle above the plume head are also observed. Note also the long-lasting effect of the plume: at 30 Myr small-scale convective movements and RT instabilities below the area affected by the plume are still vigorous. Actually, the post-plume relaxation continues in this case during 70-100 Myr. b) Similar experiment but for the case when the thickness of cratonic blocks exceeds that of the normal lithosphere only by 25 km. It illustrates the crucial role of the cratonic blocks in the experiment of Figure 5a: without essentially thick cratonic “barriers” the plume erodes away the mantle lithosphere very rapidly (at 12 Myr, all the affected area is thinned). c) “Cold” experiment similar to one shown in Figure 5a but assuming whole mantle convection geotherm: temperature boundary condition at 650 km is 1750°C (Burov and Cloetingh, 2009).

Figure 6: Some characteristic return (retrograde) P-T-t paths extracted from the model near the inner borders of the cratonic blocks (see sketch on top, and black dots in Figure 5a, temperature field at

time 3 Myr.) from times 0 to 20-30 Myr. Beginning of each P-T-t path corresponds to the numbered location. (1) Paths coming from the base of the lithosphere; (2) Paths coming from Moho depth; (3) Paths coming from the middle crust. Note that some HP-HT paths from the base of the lithosphere ($P=2.5$ GPa) have arrived near to middle-crustal depth (see text for uncertainties and order of magnitudes indicated on the right). In all cases only the paths that ascent to the surface (to at least middle crustal depths) were retained. We also show one of the “rotating” paths starting from near-keel zone (1) in the mantle lithosphere. Rotating paths were also observed in the other units (2,3). The existence of such paths hints that in some cases the interpretation of petrology data might be not straightforward as the usual assumption of the petrological analysis is based on the hypothesis of simple trajectories.

Figure 7: Spatial distribution of south and east African cratons (upper left), primary diamond deposits (upper right), ruby and sapphire deposits (lower left) and tin (+/- Ta, W, Li, Be) deposits (lower right). Initials of cratons: WC=West central African craton; WN=West Nile craton; Tz=Tanzanian craton; K=Kasai craton; CS(WA)=Central Shield (West Angola) craton; Z-K=Zimbabwe-Kaapvaal craton; A-A=Antananarivo-Antongil craton. See text for a more detailed description.

Figure 8: Thermobarometric data from rocks and gemstones bordering the Tanzanian craton. Dash-dotted curve shows a typical geotherm in a stable cratonic area (e.g. Jaupart and Mareschal, 1999). *A:* P-T-t path (dotted curve) for eclogites from the Usagaran and Ubende belts (Möller et al., 1995; Collins et al., 2004); *B:* P-T-t path for granulites from the western Mozambique belt (Cutten et al., 2006); *C:* P-T-t path (dashed curve) for granulites from the eastern Mozambique belt (Appel et al., 1998); *D:* P-T-t path for metapelites from eastern Mozambique belt (Sommer et al., 2008); *E:* Ultramafic granulites from Uluguru mountains, eastern Tanzania (Muhongo and Tuisku, 1996); *F:* Metagabbros from the Ubendian belt, south-western Tanzania (Muhongo et al., 2002); *G:* Ruby-bearing rocks from Southwest Madagascar (Mercier et al., 1999b); *H:* Ruby-bearing rocks from SE Kenya (Mercier et al., 1999a). *I:* Stability of Crn+Qtz (Shaw and Arima, 1998; Schenk et al., 2004) and of Crn+Grt+Cpx in ruby-bearing rocks of Madagascar (Rakotondrazafy et al., 2006); *J* and *K:* ultrahigh temperature metamorphism at southern and northern edges of Tanzanian craton (Sandiford et al., 1987; Schenk et

al., 2004). Localities of rock samples bordering the craton are indicated in the inset (data D, G and I are located out of the inset).

Figure 9: Model for plume head - cratonic blocks interactions in east Africa, from an initial superplume event (a) leading to Gondwana breakup and dispersal of the three cratonic blocks (Tanzanian, Madagascar and Dharwar); (b and c): continuous plume activity results in partial erosion of the base of cratonic blocks, either focusing plume pathways along the sloping base (left) or blocking plume heads at cratonic border (right); (d) favourable conditions for partial melting, ultrahigh temperature metamorphism and granite-related (tin) deposits establish in the left case, while gemstones, eclogites and ultrahigh pressure metamorphism are favoured in the right case; (e) drip-like instabilities result in counterclockwise P-T-t paths whereas slab-like instabilities are associated with clockwise P-T-t paths.

References

- Agard, P., Yamato, P., Jolivet, L., Burov, E., Exhumation of oceanic blueschists and eclogites in subduction zones: timing and mechanisms, *Earth Sci. Rev.*, 92, 53-79, 2009
- Arndt, N. T., Naldrett, A.J., Hunter, D.R., Ore deposits associated with mafic magmas in the Kaapvaal craton, *Mineral. Deposita*, 32, 323-334, 1997
- Appel, P., Möller, A., Schenk, V., High-pressure granulite facies metamorphism in the Pan-African belt of eastern Tanzania: P-T-t evidence against granulite formation by continent collision, *J. Metamorph. Geol.*, 16, 491-509, 1998
- Bouhallier, H., Chardon, D., Choukroune, P., Strain patterns in Archean dome-an-basin structures: the Dharwar craton (Karnataka, South India), *Earth Planet. Sci. Lett.*, 135, 57-75
- Boyd, F.R., Gurney, J.J., Richardson, S.H., Evidence for a 150–200 km thick Archaean lithosphere from diamond inclusion thermobarometry, *Nature* 315, 387– 389, 1985
- Brown, M., From microscope to mountain belt: 150 years of petrology and its contribution to understanding geodynamics, particularly the tectonics of orogens, *J. Geodyn.*, 32, 115-164, 2001
- Brown, M., Hot orogens, tectonic swithching, and creation of continental crust: comment, *Geology*, 31, e9, 2003
- Burov, E.B., Molnar, P., Gravity Anomalies over the Ferghana Valley (central Asia) and intracontinental Deformation, *J. Geophys. Res.*, 103,18137-18152, 1998
- Burov, E., Jaupart, C., Guillou-Frottier, L., Ascent and emplacement of buoyant magma bodies in brittle-ductile upper crust, *J. Geophys. Res.*, v. 108, B4, 2177, doi:10.1029/2002JB001904, 2003.
- Burov, E., Guillou-Frottier, L., The plume head – continental lithosphere interaction using a tectonically realistic formulation for the lithosphere, *Geophys. J. Int.*, 161, 469-490, 2005
- Burov, E., Guillou-Frottier, L., d'Acremont, E., Le Pourhiet, L., Cloetingh, S., Plume head – lithosphere interactions near intra-continental plate boundaries, *Tectonophysics*, 434, 15-38, 2007
- Burov, E. and Cloetingh, S., Controls of mantle plumes and lithospheric folding on modes of intraplate continental tectonics: differences and similarities, *Geophys. J. Int.*, 178, 1691-1722, 2009
- Camp, V.E., Hanan, B.B., A plume-triggered delamination origin for the Columbia River Basalt Group, *Geosphere*, 4, 480-495, 2008

- Chakrabarti, R., Basu, A.R., Santo, A.P., Tedesco, D., Vaselli, O., Isotopic and geochemical evidence for a heterogeneous mantle plume origin of the Virunga volcanics, Western rift, East African Rift system, *Chem. Geol.*, 259, 273-289, 2009
- Chardon, D., Choukroune, P., Jayananda, M., Sinking of the Dharwar basin (south India): implications for Archaean tectonics, *Precamb. Res.*, 91, 15-39, 1998
- Collins, W.J., Hot orogens, tectonic switching, and creation of continental crust, *Geology*, 30, 535-538, 2002
- Collins, W.J., Hot orogens, tectonic switching, and creation of continental crust: reply, *Geology*, 31, e10, 2003
- Collins, A.S., Reddy, S.M., Buchan, C., Mruma, A., Temporal constraints on Palaeoproterozoic eclogites formation and exhumation (Usagaran Orogen, Tanzania), *Earth Planet. Sci. Lett.*, 224, 175-192, 2004
- Coltice, N., Phillips, B.R., Bertrand, H., Ricard, Y., Rey, P., Global warming of the mantle at the origin of flood basalts over supercontinents, *Geology*, 35, 391-394, 2007
- Condie, K.C., Continental growth during a 1.9 Ga superplume event, *J. Geodyn.*, 34, 249-264, 2002
- Connolly, J.A.D. Computation of phase equilibria by linear programming: a tool for geodynamic modeling and its application to subduction zone decarbonation. *Earth and Planet. Sci. Lett.* 236, 524-541, 2005.
- Corti, G., van Wijk, J., Cloetingh, S., Morley, C.K., Tectonic inheritance and continental rift architecture: numerical and analogue models of the East African Rift system, *Tectonics*, 26, TC6006, doi:10.1029/2006TC002086, 1-13, 2007
- Crough, S.T., Thermal origin of mid-plate hot-spot swells, *Geophys. J. Roy. Astron. Soc.*, 55, 451-469, 1978.
- Cutten, H., Johnson, S.P., De Waele, B., Protolith ages and timing of metasomatism related to the formation of whiteschists at Mautia Hill, Tanzania: implications for the assembly of Gondwana, *J. Geol.*, 114, 683-698, 2006
- d'Acremont, E., Leroy, S., Burov, E., Numerical modelling of a mantle plume: the plume head - lithosphere interaction in the formation of an oceanic large igneous province, *Earth Planet. Sci. Lett.*, 206, 379-396, 2003

- Dziewonski, A.M., Lekic, V., Romanowicz, B.A., Mantle Anchor Structure: an argument for bottom up tectonics, *Earth Planet. Sci. Lett.*, 299, 69-79, 2010
- Ebinger, C., Djomani, Y.P., Mbede, E., Foster, A., Dawson, J.B., Rifting Archean lithosphere: the Eyasi-Manyara-Natron rifts, East Africa, *J. Geol. Soc.*, 154, 947-960, 1997
- Ebinger, C., Sleep, N.H., Cenozoic magmatism in central and east Africa resulting from impact of a one large plume, *Nature*, 395, 788-791, 1998
- Elder, J., Convective self-propulsion of continents, *Nature*, 214, 657-750, 1967
- Elkins-Tanton, L., Continental magmatism, volatile recycling, and a heterogeneous mantle caused by lithospheric gravitational instabilities, *J. Geophys. Res.*, 112, B03405, doi:10.1029/2005JB004072
- England, P., Thompson, A.B., Pressure-temperature-time paths of regional metamorphism I. Heat transfer during the evolution of regions of thickened continental crust, *J. Petrol.*, 25, 894-928, 1984
- England, P., Houseman, G., On the geodynamic setting of kimberlite genesis, *Earth Planet. Sci. Lett.*, 67, 109-122, 1984
- Forte, A.M., Mitrovica, J.X., Deep-mantle high-viscosity flow and thermochemical structure inferred from seismic and geodynamic data, *Nature*, 410, 1049-1056, 2001
- Gao, S., Rudnick, R.L., Xu, W-L., Yuan, H-L., Liu, Y-S., Walker, R.J., Puchtel, I-S., Liu, X., Huang, H., Wang, X-R., Yang, J., Recycling deep cratonic lithosphere and generation of intraplate magmatism in the North China craton, *Earth Planet. Sci. Lett.*, 270, 41-53, 2008
- Giuliani, G., Fallick, A., Rakotondrazafy, M., Ohnenstetter, D., et al, Oxygen isotope systematics of gem corundum deposits in Madagascar: relevance for their geological origin, *Mineral. Deposita*, 42, 251-270, 2007
- Guillou, L., Jaupart, C., On the effect of continents on mantle convection, *J. Geophys. Res.*, 100, 24,217-24,238, 1995
- Guillou-Frottier, L., Burov, E., Nehlig, P., Wyns, R., Deciphering plume-lithosphere interactions beneath Europe from topographic signatures, *Global Planet. Change*, 58, 119-140, 2007
- Gurnis, M., Mitrovica, J.X., Ritsema, J., van Heijst, H-J., Constraining mantle density structure using geological evidence of surface uplift rates: the case of the African superplume, *Geochem. Geophys. Geosys.*, 1, 2000.

- Halpin, J.A., Clarke, G.L., White, R.W., Kelsey, D.E., Contrasting P-T-t paths for Neoproterozoic metamorphism in McRobertson and Kemp Lands, east Antarctica, *J. Metamorphic Geol.*, 25, 683-701, 2007
- Hewitt, J.M., McKenzie, D.P., Weiss, N.O., Large aspect ratio cells in two-dimensional thermal convection, *Earth Planet. Sci. Lett.*, 51, 370-380, 1980
- Houseman, G., McKenzie, D.P., Molnar, P., Convective instability of a thickened boundary layer and its relevance for the thermal evolution of continental convergent belts, *J. Geophys. Res.*, 86, 6115-6132, 1981.
- Houseman, G.A., Molnar, P., Gravitational (Rayleigh-Taylor) instability of a layer with non-linear viscosity and convective thinning of continental lithosphere, *Geophys. J. Int.*, 128, 125-150, 1997
- Jaupart, C., Mareschal, J.-C., The thermal structure and thickness of continental roots, *Lithos*, 48, 93-114, 1999
- Jellinek, M.A., Manga, M., Links between long-lived hotspots, mantle plumes, D" and plate tectonics, *Rev. Geophys.*, 42,3, RG3002, doi:10.1029/2003RG000144, 2004
- Kabongo, E.K., Sebagenzi, S.M.N., Lucazeau, F., A Proterozoic-rift origin for the structure and the evolution of the cratonic Congo basin, *Earth Planet. Sci. Lett.*, 304, 240-250, 2011.
- Kelsey, D.E., On ultrahigh-temperature crustal metamorphism, *Gondwana Res.*, 13, 1-29, 2008
- Koulakov, I., Kaban, M.K., Tesauro, M., Cloetingh, S., P- and S-velocity anomalies in the upper mantle beneath Europe from tomographic inversion of ISC data, *Geophys. J. Int.*, 179, 345-366, 2009
- Kusky T.M., Polat, A., Growth of granite-greenstone terranes at convergent margins, and stabilization of Archean cratons, *Tectonophysics*, 305, 43-73, 1999
- Le Goff, E., Deschamps, Y., Muhongo, S., Cocherie, A., Milesi, J.-P., Pinna, P., Msechu, M., Msihili, A., The Tanzanian "Ruby Belt": structural, petrological and geochronological constraints within the pan-African orogeny – examples from the Morogoro and Mahenge districts, *Colloquium of African Geology*, CAG20, Orléans, France, 2-7 June 2004
- Le Goff, E., Deschamps, Y., Guerrot, C., Tectonic implications of new single zircon Pb-Pb evaporation data in the Lossogonoi and Longido ruby-districts, Mozambican metamorphic Belt of north-eastern Tanzania, *C. R. Geosc.*, 342, 36-45, 2010

- Lenardic, A., Moresi, L.-N., Mühlhaus, H., Longevity and stability of cratonic lithosphere: insights from numerical simulations of coupled mantle convection and continental tectonics, *J. Geophys. Res.*, 108, 2303, doi:10.1029/2002JB001859, 2003
- Lenardic, A., Moresi, L.-N., Jellinek, A.M., Manga, M., Continental insulation, mantle cooling, and the surface area of oceans and continents, *Earth Planet. Sci. Lett.*, 234, 317-333, 2005
- Malisa, E., Muhongo, S., Tectonic setting of gemstone mineralization in the Proterozoic metamorphic terrane of the Mozambique belt of Tanzania, *Precamb. Res.*, 46, 167-176, 1990
- Mercier, A., Debat, P., Saul, J.M., Exotic origin of the ruby deposits of the Mangari area in SE Kenya, *Ore Geol. Rev.*, 14, 83-104, 1999a
- Mercier, A., Rakotondrazafy, M., Ravolomandrinarivo, B., Ruby mineralization in southwest Madagascar, *Gondwana Res.*, 2, 433-438, 1999b
- Milesi, J-P., Feybesse, J-L., Pinna, P., Deschamps, Y., Kampuzu, A.B., Muhongo, S., Lescuyer, J-L., Le Goff, E., Delor, C., Billa, M., Ralay, F., Henry, C., Géologie et principaux gisements d'Afrique, carte et SIG à 1:10,000,000, *Colloquium of African Geology, CAG20*, Orléans, France, 2-7 june 2004
- Milesi, J.-P., Toteu, S.F., Deschamps, Y., et al., An overview of the geology and major ore deposits of Central Africa : explanatory note for the 1 :4,000,000 map « geology and major ore deposits of Central Africa », *J. Afr. Earth Sci.*, 44, 571-595, 2006
- Möller, A., Appel, P., Mezger, K., Schenk, V., Evidence for a 2 Ga subduction zone: eclogites in the Usagaran belt of Tanzania, *Geology*, 23, 1067-1070, 1995
- Möller, A., Mezger, K., Schenk, V., U-Pb dating of metamorphic minerals: Pan-African metamorphism and prolonged slow cooling of high pressure granulites in Tanzania, east Africa, *Precamb. Res.*, 104, 123-146, 2000
- Montagner, J-P., Marty, B., Stutzmann, E., Sicilia, D., Cara, M., Pik, R., Lévêque, J-J., Rault, G., Beucler, E., Debayle, E., Mantle upwellings and convective instabilities revealed by seismic tomography and helium isotope geochemistry beneath east Africa, *Geophys. Res. Lett.*, 34, L21303, doi:10.1029/2007GL031098, 2007
- Montelli, R., Nolet, G., Dahlen, F.A., Masters, G., Engdahl, E.R., Hung, S-H., Finite frequency tomography reveals a variety of plumes in the mantle, *Science*, 303, 338-343, 2004

- Muhongo, S., Tuisku, P., Pan-African high pressure isobaric cooling: evidence from the mineralogy and thermobarometry of the granulite-facies rocks from the Uluguru mountains, eastern Tanzania, *J. Afr. Earth Sci.*, 1996
- Muhongo, S., Tuisku, P., Mnali, S., Temu, E., Appel, P., Stendal, H., High-pressure granulite-facies metagabbros in the Ubendian belt of SW Tanzania: preliminary petrography and P-T estimates, *J. Afr. Earth Sci.*, 34, 279-285, 2002
- Nyblade, A.A., Owens, T.J., Gurrola, H., Ritsema, J., Langston, C.A., Seismic evidence for a deep upper mantle thermal anomaly beneath east Africa, *Geology*, 28, 599-602, 2000
- Olson, P., Hot spots, swells and mantle plumes, in: Magma transport and storage, pp 33-51, M.P. Ryan (ed.), John Wiley and Sons Ltd., Chichester, U.K., 1990
- O'Neill, C.J., Moresi, L., Jaques, A.L., Geodynamic controls on diamond deposits: implications for Australian occurrences, *Tectonophysics*, 404, 217-236, 2005
- Petit, C., Ebinger, C., Flexure and mechanical behaviour of cratonic lithosphere: gravity models of the East Africa and Baikal rifts, *J. Geophys. Res.*, 105, 19151-19162, 2000
- Petrini, K., and Y. Podladchikov, Lithospheric pressure-depth relationship in compressive regions of thickened crust, *J. Metamorphic Geol.*, 18, 67-77, 2000
- Phillips, B.R., Coltice, N., Temperature beneath continents as a function of continental cover and convective wavelength, *J. Geophys. Res.*, 115, B04408, doi:10.1029/2009JB006600, 1-13, 2010
- Pirajno, F., Hotspots and mantle plumes: global intraplate tectonics, magmatism and ore deposits, *Mineral. Petrol.*, 82, 183-216, 2004
- Platt, J.P., and P.C. England Convective removal of lithosphere beneath mountain belts; thermal and mechanical consequences, *Amer. J. Sci.*, 294, 307-336, 1994.
- Pouradier, A., Sig Afrique: magmatisme alcalin et carbonatitique et minéralisations en métaux rares associés, unpublished MSc. Thesis, 2002
- Prakash, D., Prakash, S., Sachan, H.K., Petrological evolution of the high pressure and ultrahigh-temperature mafic granulites from Karur, southern india: evidence for decompressive and cooling retrograde trajectories, *Miner. Petrol.*, 100, 35-53, 2010
- Pysklywec, R.N., Shahnas, M.H., Time-dependent surface topography in a coupled crust-mantle convection model, *Geophys. J. Int.*, 154, 268-278, 2003

- Rakotondrazafy, A.F.M., Giuliani, G., Razanatseheno, M., Moine, B., Saholy, R., Théogene, R.L., Alfred, A.S., Petrographie des roches à rubis et à saphir du socle cristallin métamorphique et des basaltes alcalins de Madagascar, *Colloquium of African Geology*, CAG21, Maputo, Mozambique, 3-5 July 2006
- Richardson, S.H., Shirey, S.B., Harris, J.W., Episodic diamond genesis at Jwaneng, Botswana, and implications for Kaapvaal craton evolution, *Lithos*, 77, 143-154, 2004
- Ritsema, J., Nyblade, A.A., Owens, T.J., Langston, C.A., VanDecar, J.C., Upper mantle seismic velocity structure beneath Tanzania, east Africa: implications for the stability of cratonic lithosphere, *J. Geophys. Res.*, 103, 21201-21213, 1998.
- Ritter, J.R.R., Jordan, M., Christensen, U.R., Achauer, U., A mantle plume below the Eifel volcanic fields, Germany, *Earth Planet. Sci. Lett.*, 186, 7-14, 2001
- Romanowicz, B., Gung, Y., Superplumes from the core-mantle boundary to the lithosphere: implications for heat flux, *Science*, 296, 513-516, 2002
- Ruppel, C., Hodges, K.V., Pressure-temperature-time paths from two-dimensional thermal models: prograde, retrograde, and inverted metamorphism, *Tectonics*, 13, 17-44, 1994
- Saleeby, J., Ducea, M., Clemens-Knott, D., Production and loss of high-density batholithic root, southern Sierra Nevada, California, *Tectonics*, 22(6), 1064, doi:10.1029/2002TC001374, 2003.
- Sandiford, M., Neall, F.B., Powell, R., Metamorphic evolution of aluminous granulites from Labwor Hills, Uganda, *Contrib. Mineral. Petrol.*, 95, 217-225, 1987
- Santosh, M., Collins, A.S., Gemstone mineralization in the Palghat-Cauvery shear zone system (Karur-Kangayam belt), southern India, *Gondwana Res.*, 6, 911-918, 2003
- Schenk, V., Cornelius, N., Schnieders, I., Ubendian ultrahigh-temperature metamorphism of metapelitic migmatites in the Songea-Mbamba bay area, southern Tanzania, *Colloquium of African Geology*, CAG20, Orléans, France, 2-7 June, 2004
- Schmitz, M.D., Bowring, S.A., Ultrahigh-temperature metamorphism in the lower crust during Neoproterozoic Ventersdorp rifting and magmatism, Kaapvaal craton, southern Africa, *Geol. Soc. Am. Bull.*, 115, 533-548, 2003
- Schubert, G., Turcotte, D.L., Olson, P., Mantle convection in the Earth and planets, Cambridge Univ. Press, U.K., 956 p., 2001

- Şengör, A.M.C., Ozeren, S., Genç, T., Zor, E., East Anatolian high plateau as a mantle-supported, north-south shortened domal structure, *Geophys. Res. Lett.*, 30, 24, 8045, 2003
- Shaw, R.K., Arima, M., A corundum-quartz assemblage from the Eastern Ghats Granulite belt, India: evidence for high P-T metamorphism?, *J. Metamorph. Geol.*, 16, 189-196, 1998
- Silver, P.G., Behn, M.D., Kelley, K., Schmitz, M., Savage, B., Understanding cratonic flood basalts, *Earth Planet. Sci. Lett.*, 245, 190-201, 2006
- Simonet, C., Geologie des gisements de saphir et de rubis. L'exemple de la John Saul Ruby mine, Mangare, Kenya, PhD. Thesis, Univ. Nantes, www.kasigau.fr/pages/thesispag.html, 344pp. 2000
- Simonet, C., Paquette, J.L., Pin, C., Lasnier, B., Fritsch, E., The Dusi (Garba tula) sapphire deposit, central Kenya - a unique Pan-African corundum-bearing monzonite, *J. Afric. Earth Sci.*, 38, 401-410, 2004
- Sleep, N.H., Ebinger, C.J., Kendall, J.-M., Deflection of mantle plume material by cratonic keels, *Geol. Soc. London Spec. Pub.*, 199, 135-150, 2002
- Smithies, R.H., Champion, D.C., Cassidy, K.F., Formation of Earth's early Archean continental crust, *Precamb. Res.*, 127, 89-101, 2003
- Sommer, H., Hauzenberger, C., Kröner, A., Muhongo, S., Isothermal decompression history in the "Western Granulite" terrane, central Tanzania: evidence from reaction textures and trapped fluids in metapelites, *J. Afric. Earth Sci.*, 51, 123-144, 2008
- Sutherland, F.L., Hoskin, P.O.W., Fanning, C.M., Coenraads, R.R., Models of corundum origin from alkali basalts terrains: a reappraisal, *Contrib. Mineral. Petr.*, 133, 356-372, 1998
- Sutherland, F.L., Fanning, C.M., Gem-bearing basaltic volcanism, Barrington, New South Wales: Cenozoic evolution, based on basalt K-Ar ages and zircon fission track and U-Pb isotope dating, *Austral. J. Earth Sci.*, 48, 221-237, 2001.
- Teixeira, J.B.G., Misi, A., da Gloria da Silva, M., Supercontinent evolution and the Proterozoic metallogeny of South America, *Gondwana Res.*, 11, 346-361, 2007
- Trubitsyn, V.P., Mooney, W.D., Abbott, D.H., Cold cratonic roots and thermal blankets: how continents affect mantle convection, *Int. Geol. Rev.*, 45, 479-496, 2003

- Van Thienen, P., van den Berg, A.P., de Smet, J.H., van Hunen, J., Drury, M.R., Interaction between small-scale mantle diapirs and a continental root, *Geochem. Geophys. Geosyst.*, 4, 8301, doi:10.1019/2002GC000338, 2003
- Walker, K.T., Nyblade, A.A., Klemperer, S.L., Bokelmann, G.H.R., Owens, T.J., On the relationship between extension and anisotropy: constraints from shear wave splitting across the East African plateau, *J. Geophys. Res.*, 109, B08302, doi:10.1029/2003JB002866, 2004
- Wallner, H., Schmeling, H., Rift induced delamination of mantle lithosphere and crustal uplift: a new mechanism for explaining Rwenzori Mountains' extreme elevation ?, *Int. J. Earth Sci.*, 99, 1511-1524, 2010
- Warren, R.G., Ellis, D.J., Mantle underplating, granite tectonics, and metamorphic P-T-t paths, *Geology*, 24, 663-666, 1996
- Weeraratne, D.S., Forsyth, D.W., Fisher, K.M., Nyblade, A.A., Evidence for an upper mantle plume beneath the Tanzanian craton from Rayleigh wave tomography, *J. Geophys. Res.*, 108, 2427, doi:10.1029/2002JB002273, 2003
- Yui, T-F., Zaw, K., Limtrakun, P., Oxygen isotope composition of the Denchai sapphire, Thailand: a clue to its enigmatic origin, *Lithos*, 153-161, 2003
- Zhang, M., O'Reilly, S.Y., Wang, K-L., Hronsky, J., Griffin, W.L., Flood basalts and metallogeny: the lithospheric mantle connection, *Earth Sci. Rev.*, 86, 145-174, 2008
- Zhao, D., Global tomographic images of mantle plumes and subducting slabs: insights into deep Earth dynamics, *Phys. Earth Planet. Int.*, 146, 3-34, 2004

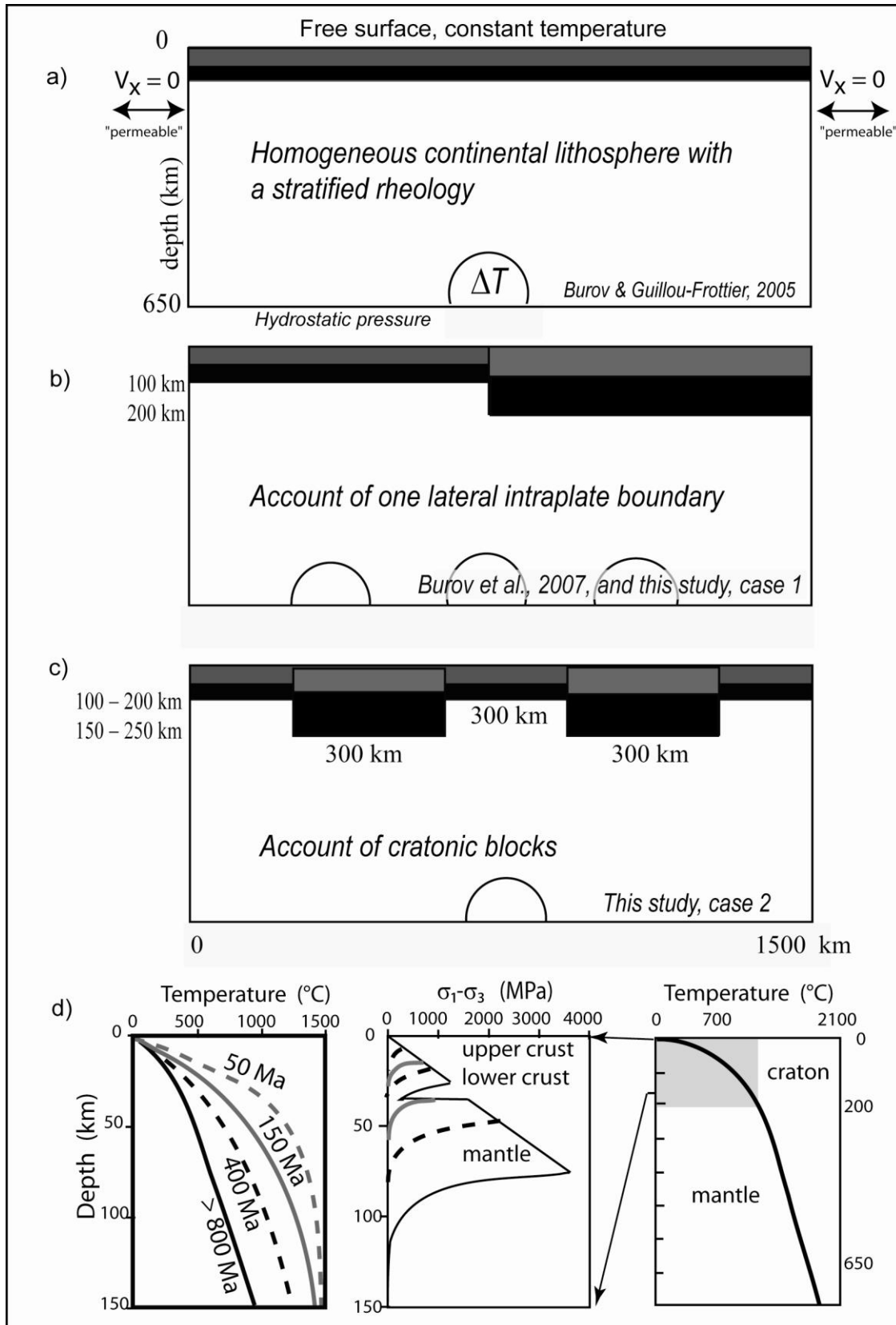


Fig. 1

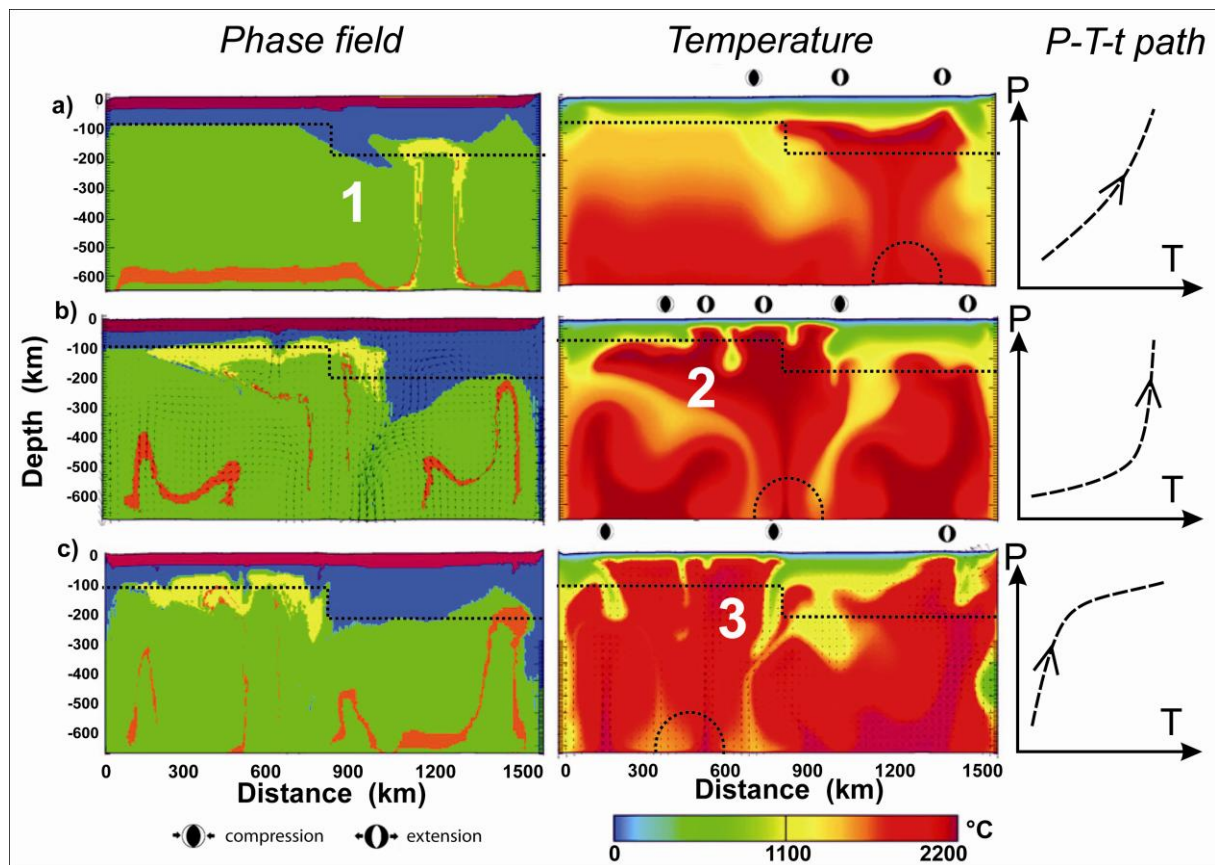


Fig. 2

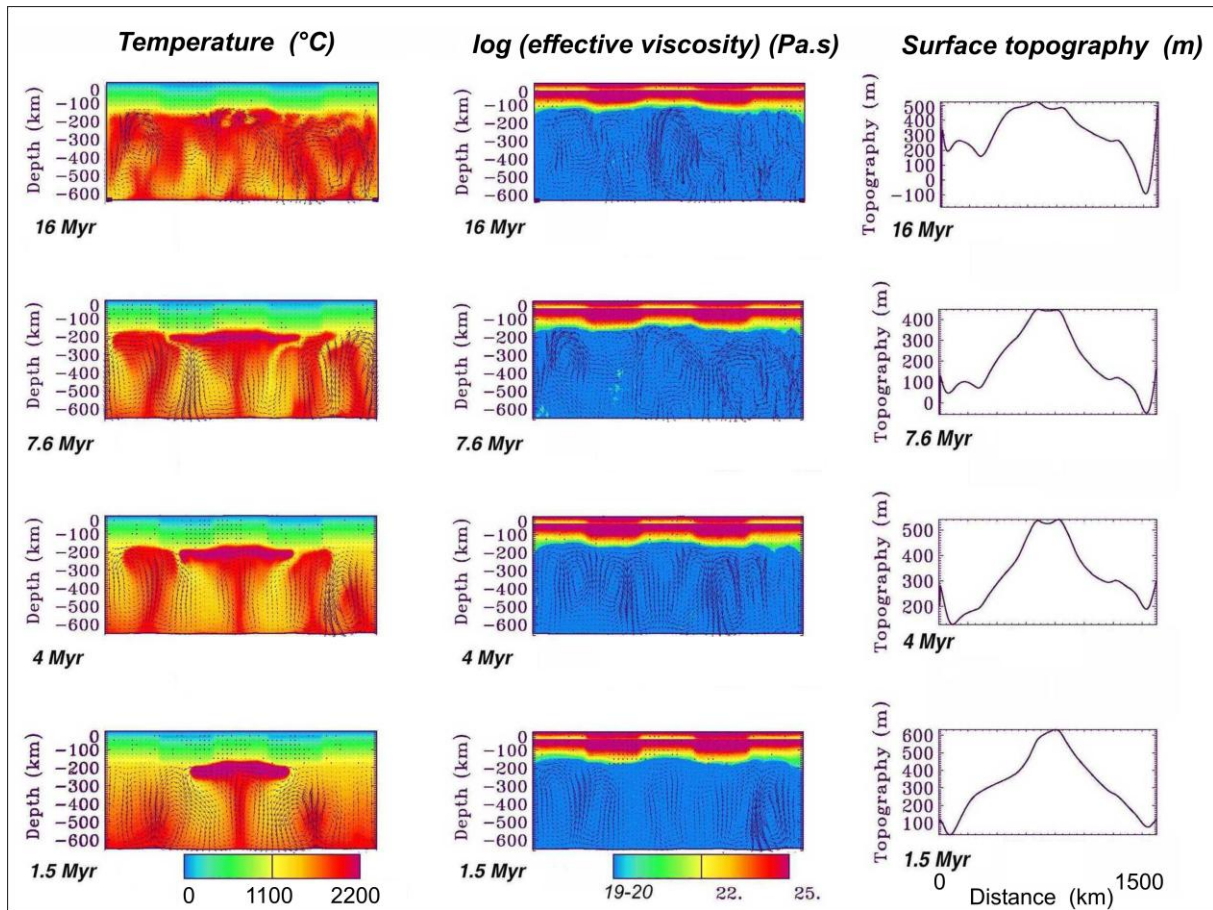


Fig. 3

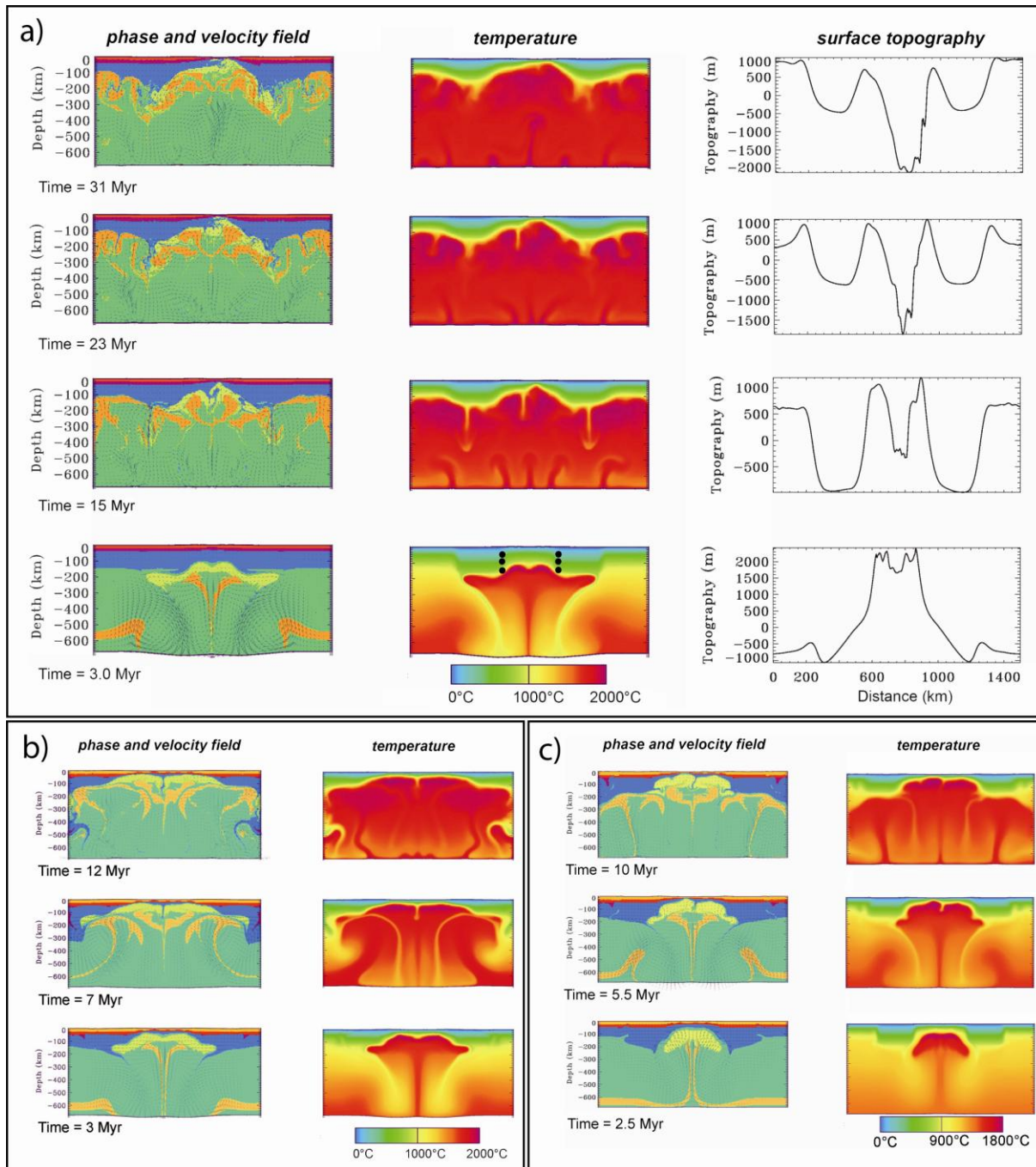


Fig. 5

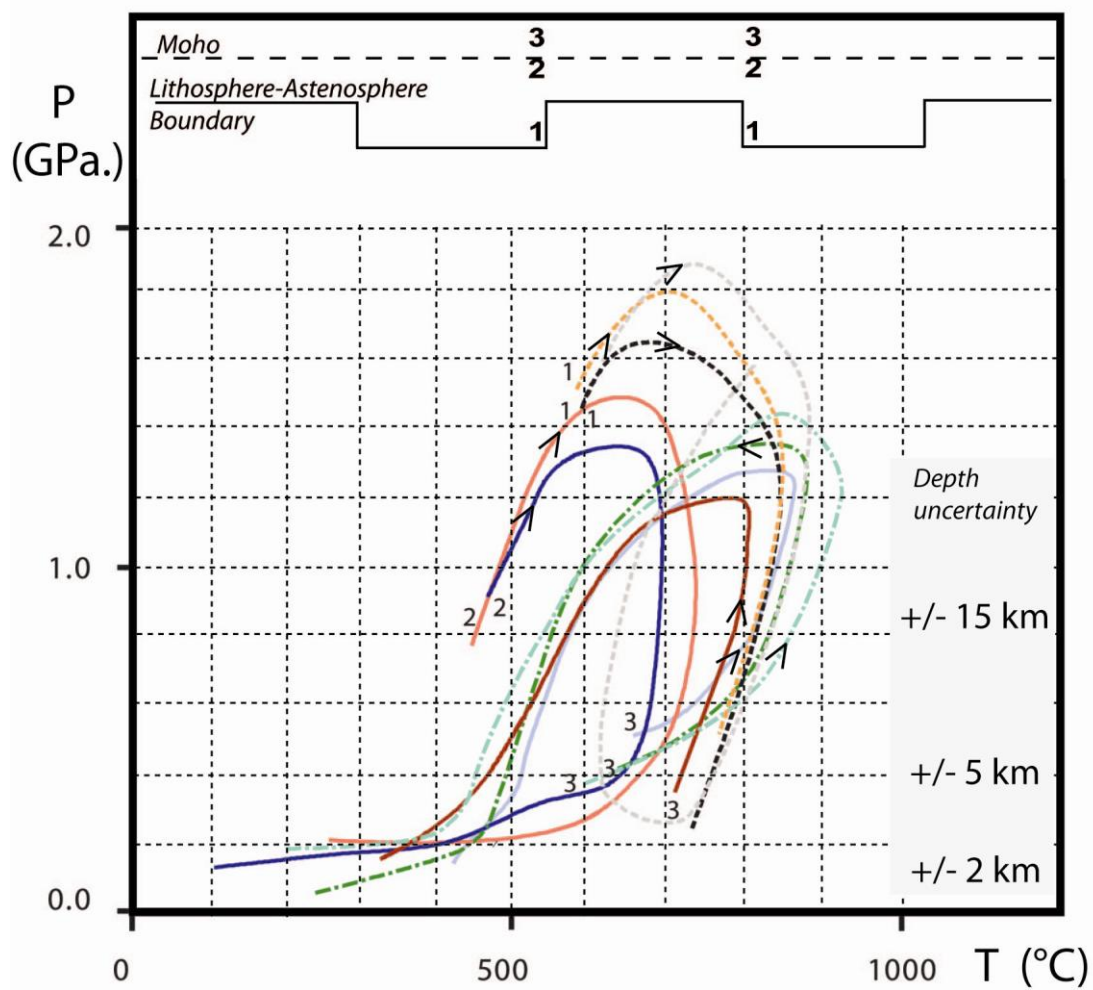


Fig. 6

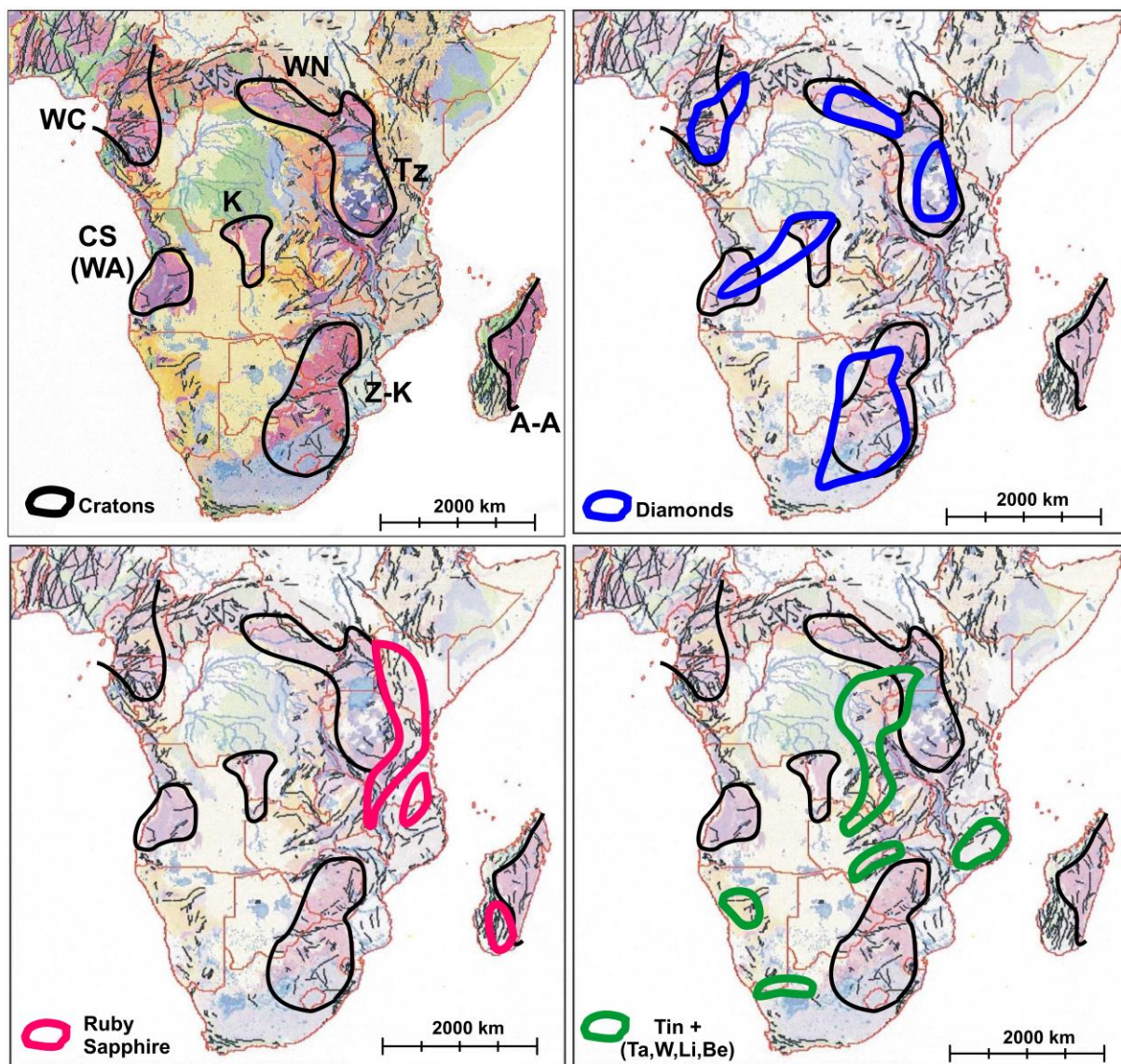


Fig. 7

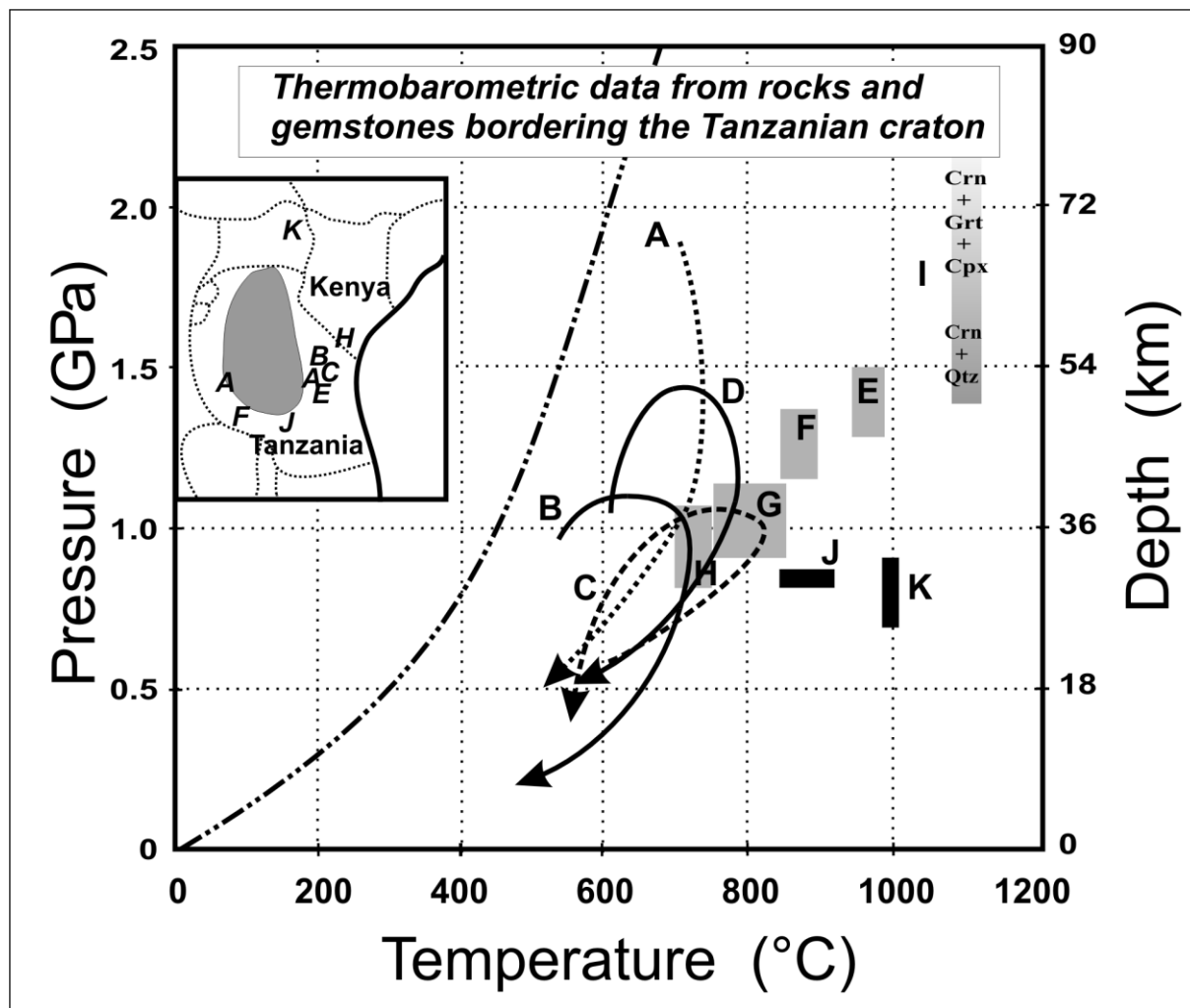


Fig. 8

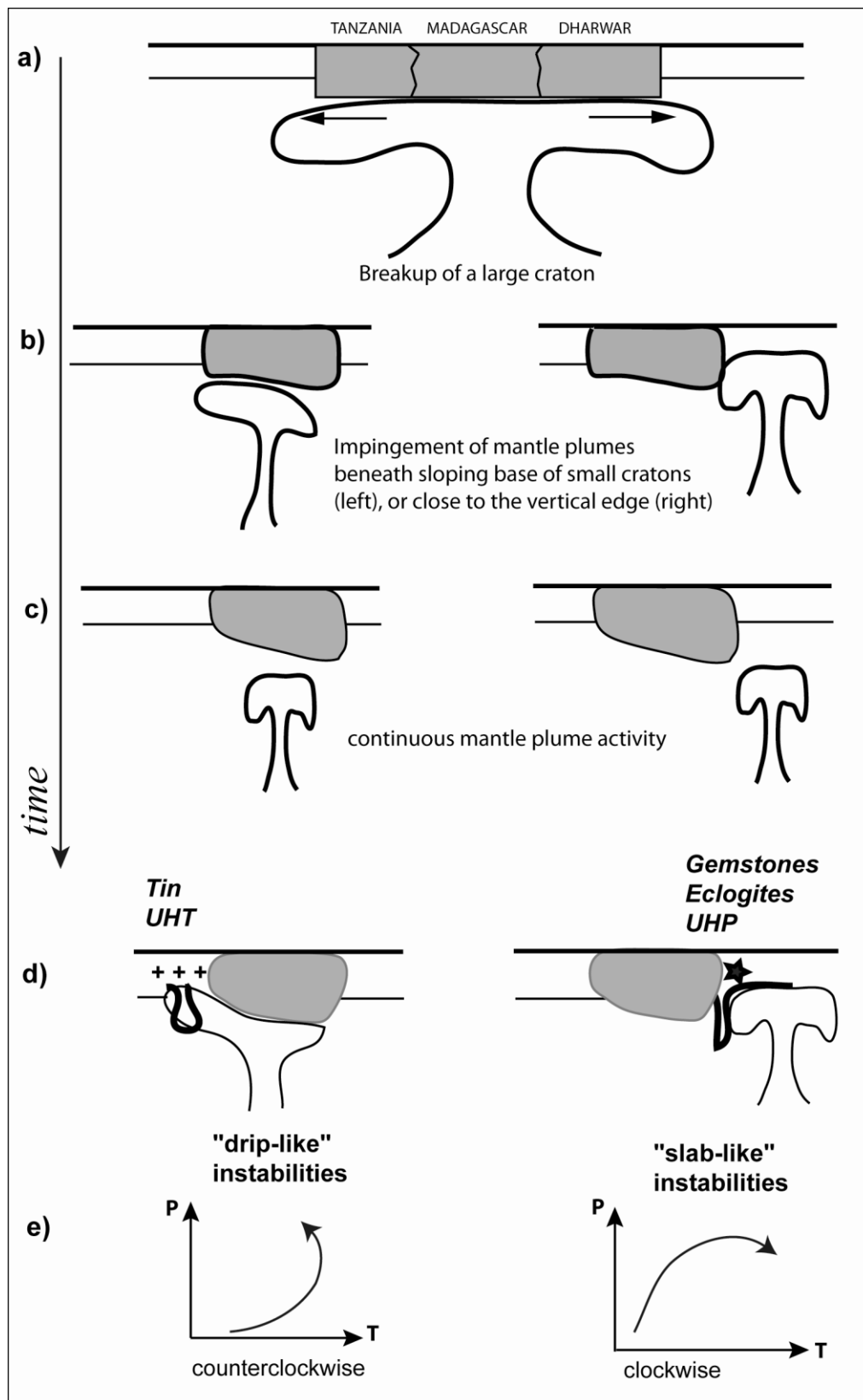


Fig. 9